Development 139, 488-497 (2012) doi:10.1242/dev.070763

Notch signaling modulates proliferation and differentiation of intestinal crypt base columnar stem cells

Kelli L. VanDussen[1], Alexis J. Carulli[1], Theresa M. Keeley[1], Sanjeevkumar R. Patel[2], Brent J. Puthoff[3], Scott T. Magness[3], Ivy T. Tran[4], Ivan Maillard[2,4,5], Christian Siebel[6], Åsa Kolterud[5], Ann S. Grosse[5], Deborah L. Gumucio[5], Stephen A. Ernst[5], Yu-Hwai Tsai[7], Peter J. Dempsey[1,7] and Linda C. Samuelson[1,2,*]

SUMMARY

Notch signaling is known to regulate the proliferation and differentiation of intestinal stem and progenitor cells; however, direct cellular targets and specific functions of Notch signals had not been identified. We show here in mice that Notch directly targets the crypt base columnar (CBC) cell to maintain stem cell activity. Notch inhibition induced rapid CBC cell loss, with reduced proliferation, apoptotic cell death and reduced efficiency of organoid initiation. Furthermore, expression of the CBC stem cell-specific marker *Olfm4* was directly dependent on Notch signaling, with transcription activated through RBP-Jκ binding sites in the promoter. Notch inhibition also led to precocious differentiation of epithelial progenitors into secretory cell types, including large numbers of cells that expressed both Paneth and goblet cell markers. Analysis of Notch function in *Atoh1*-deficient intestine demonstrated that the cellular changes were dependent on *Atoh1*, whereas Notch regulation of *Olfm4* gene expression was *Atoh1* independent. Our findings suggest that Notch targets distinct progenitor cell populations to maintain adult intestinal stem cells and to regulate cell fate choice to control epithelial cell homeostasis.

KEY WORDS: Olfactomedin 4, Lgr5, Atoh1, Gamma-secretase inhibitor, Tuft cell, Mouse

INTRODUCTION

The intestinal epithelium is continuously replenished from stem and progenitor cell populations located in the crypts. Recent studies have identified an actively dividing stem cell, termed the crypt base columnar (CBC) stem cell, as a self-renewing progenitor responsible for maintaining the epithelium (Barker et al., 2007). Although the CBC stem cell was originally described many decades ago based on its unique cellular morphology (Cheng and Leblond, 1974b; Cheng and Leblond, 1974a), the more recent identification of CBC stem cell markers, including *Lgr5*, *Ascl2* and *Olfm4* (Barker et al., 2007; van der Flier et al., 2009), has greatly facilitated the study of this stem cell population. Replicating CBC stem cells can self-renew or give rise to rapidly dividing transit-amplifying (TA) cells, which are short-lived progenitors that differentiate into mature cell types, including absorptive enterocytes, hormone-secreting enteroendocrine cells, mucus-secreting goblet cells, antimicrobial peptide-secreting Paneth cells and chemosensing tuft cells (Barker et al., 2007; Gerbe et al., 2011). The factors regulating stem cell self-renewal versus differentiation are not well understood, although competition for limited niche binding sites has been proposed to control total CBC stem cell number (Snippert et al., 2010).

The role of Notch signaling in the regulation of both progenitor cell proliferation and cellular differentiation in the intestine is well established; Notch signaling promotes differentiation to the absorptive cell lineage rather than to the secretory cell lineage (Jensen et al., 2000; Fre et al., 2005; Stanger et al., 2005; van Es et al., 2005; Riccio et al., 2008; Gerbe et al., 2011; Pellegrinet et al., 2011). Notch pathway inhibition of the transcription factor atonal homolog 1 (*Atoh1*) provides the crucial mechanism regulating cell fate choice, and *Atoh1* expression appears to be both required (Yang et al., 2001; Shroyer et al., 2007) and sufficient (VanDussen and Samuelson, 2010) for the program of secretory cell differentiation. In general, disruption of Notch signaling results in increased *Atoh1* expression and loss of proliferation coupled with secretory cell hyperplasia, whereas hyperactive Notch signaling results in decreased *Atoh1* expression and in expansion of the proliferative zone with increased numbers of absorptive enterocytes. Accordingly, genetic depletion of Notch pathway components, including the crucial Notch DNA-binding protein RBP-Jκ (Rbpj – Mouse Genome Informatics) (van Es et al., 2005), both Notch1 and Notch2 receptors (Riccio et al., 2008) or both delta-like (Dll) 1 and 4 ligands (Pellegrinet et al., 2011), results in decreased cellular proliferation in the intestinal crypts together with secretory cell hyperplasia. Similar phenotypes have been observed in rodents after treatment with γ-secretase inhibitors (GSIs) (Milano et al., 2004; Wong et al., 2004; van Es et al., 2005), which block an essential protein cleavage event in the activation of Notch signaling, or with a combination of neutralizing antibodies specific for the Notch1 and Notch2 receptors (Wu et al., 2010). Conversely, activation of constitutive Notch signaling in the mouse intestinal epithelium expands the proliferative zone and represses secretory cell differentiation (Fre et al., 2005; Stanger et al., 2005).

Notch is likely to target distinct stem and progenitor cell populations to regulate different aspects of intestinal homeostasis, although specific cellular targets had not been definitively identified. Crucial components of the Notch signaling pathway, including the Notch1 and Notch2 receptors, the ligands jagged 1, Dll1 and Dll4, and the Notch target genes hairy and enhancer of split 1 (*Hes1*), *Hes5* and *Hes6*, have been localized to the proliferative zone of the

Departments of [1]Molecular & Integrative Physiology, [2]Internal Medicine, [5]Cell & Developmental Biology and [7]Pediatrics & Communicable Diseases, and [4]The Life Sciences Institute, The University of Michigan, Ann Arbor, MI 48109, USA. [3]Departments of Medicine and Biomedical Engineering, The University of North Carolina at Chapel Hill, Chapel Hill, NC 27599, USA. [6]Department of Molecular Biology, Genentech, San Francisco, CA 94080, USA.

*Author for correspondence (lcsam@umich.edu)

Accepted 29 November 2011

intestinal crypts (Jensen et al., 2000; Schroder and Gossler, 2002; Benedito and Duarte, 2005; Crosnier et al., 2005; van Es et al., 2005; Riccio et al., 2008). Importantly, lineage tracing from cells undergoing active Notch signaling identified long-lived progenitors that gave rise to all the mature epithelial cell types (Vooijs et al., 2007; Pellegrinet et al., 2011), suggesting that Notch signaling was active in a stem cell. More specifically, Notch regulation of the CBC stem cell was suggested by the enrichment of *Notch1* receptor mRNA in this cell type (van der Flier et al., 2009).

Although these studies build a strong case for the idea that the Notch pathway is active in adult intestinal stem cells, the significance of this signaling pathway for stem cell function is unknown. In this study, we demonstrate that Notch signaling in CBC stem cells is required for stem cell proliferation and survival. Furthermore, we demonstrate that Notch regulation of the CBC stem cell is *Atoh1* independent, whereas Notch regulation of epithelial cell fate is *Atoh1* dependent, suggesting that Notch targets distinct aspects of progenitor cell function to regulate intestinal epithelial cell homeostasis.

MATERIALS AND METHODS

Mice

C57BL/6 mice were used unless otherwise noted. *Atoh1*$^{lacZ/lacZ}$ (Yang et al., 2001) (gift from N. F. Shroyer), *Lgr5-EGFP-IRES-creERT2* (*Lgr5-GFP*) (Barker et al., 2007) (Jackson Laboratories, #008875), Vil-Cre (Pinto et al., 1999) and *Rosa*^{NotchIC} (Murtaugh et al., 2003) (Jackson Laboratories, #008159) mice were genotyped by PCR as recommended by the Jackson Laboratory or with the primers listed in supplementary material Table S1. Mice were maintained specific pathogen-free under a 12-hour light cycle and protocols were approved by the University of Michigan Committee on the Use and Care of Animals.

Notch inhibition

Administration of dibenzazepine (DBZ; SYNCOM, Groningen, The Netherlands) was as described (van Es et al., 2005). Mice aged 2 months were injected intraperitoneally (i.p.) (30 μmol/kg DBZ or vehicle daily) for 5 days and fasted overnight before tissue collection on day 6.

A mixture of neutralizing antibodies directed against the Notch1 and Notch2 receptors was administered by i.p. injection to BALB/c mice at 5 mg/kg on days 1 and 4 with tissue collection on day 6 as described (Wu et al., 2010). An irrelevant anti-HSV gD (GD) humanized antibody was used as a control.

Fetal intestine organ culture

The morning of the vaginal plug was considered embryonic day (E) 0.5. For organ culture, E15.5 intestine segments (A-D, proximal to distal) were cultured at the air-liquid interface on Transwell plates (Costar 3428) in BGJ/b media (Gibco) with 0.1 mg/ml ascorbic acid (Sigma) and Pen-Strep (Gibco). GSI (DAPT; EMD4Biosciences, Gibbstown, NJ, USA) was added at 40 μM unless otherwise indicated, and cultures were incubated for up to 4 days with daily media changes.

Bromodeoxyuridine (BrdU) administration and tissue collection

Adult mice were injected with 50 mg/kg BrdU (5 mg/ml in 0.9% saline; Sigma) 2 hours prior to tissue collection. Intestine was dissected as follows: duodenum (4 cm distal to pylorus), jejunum (4 cm at the midpoint), ileum (4 cm proximal to cecum) and colon (4 cm distal to cecum). The proximal 1 cm of each tissue segment was processed for paraffin embedding after fixation in 4% PBS-buffered paraformaldehyde at 4°C overnight. Fetal organ culture segments A and D were similarly processed for paraffin embedding. Duodenal tissue was collected from newborn Vil-Cre; *Rosa*^{NotchIC} mice and processed for RNA collection.

Histological analysis

Paraffin sections (5 μm) were stained with periodic acid-Schiff (PAS)/Alcian Blue (Newcomer Supply, Middleton, WI, USA) to assess mucin-containing goblet cells. Immunostaining was performed as described (Lopez-Diaz et al., 2006). Primary antibodies were used as described (Keeley and Samuelson, 2010; VanDussen and Samuelson, 2010) or as follows: goat anti-CgA (1:100, Santa Cruz), rabbit anti-DCAMKL1 (1:50, Abcam), chicken anti-GFP (1:700, Aves Labs), rabbit anti-Ki67 (Thermo Scientific, 1:200), rat anti-Mmp7 (1:100) (Fingleton et al., 2007) and rabbit anti-Sox9 (1:150, Millipore). For immunofluorescence, secondary antibodies (1:400; Invitrogen or Jackson ImmunoResearch) conjugated to Alexa Fluor 488, Alexa Fluor 555, FITC or Cy3 were combined with DAPI nuclear stain (ProLong Gold, Invitrogen). For Ki67 and Sox9 staining, antigen retrieval was performed with Triology solution (Cell Marque, Rocklin, CA, USA). Microscopy was performed with a Nikon E800 or Olympus BX-51 equipped with a SPOT or Olympus DP70 digital camera, respectively. Confocal microscopy was performed with an Olympus FV500. For morphometric analysis of CBC stem cells, jejunum sections from *Lgr5-GFP* mice were co-stained for Ki67 and GFP. A total of 1673 and 1562 crypts were counted from vehicle-treated (n=4) and DBZ-treated (n=4) mice, respectively.

For electron microscopy, jejunum and ileum from three mice from each treatment group were evaluated. Small transverse sections of intestine were fixed for 2 hours in 2% glutaraldehyde and 2% formaldehyde (prepared fresh from paraformaldehyde) in PBS, postfixed for 45 minutes with 1% OsO_4, dehydrated and Epon embedded. Ultrathin sections were stained with uranyl acetate and lead citrate, and at least ten images were recorded digitally for each intestine using a Philips CM-100 electron microscope.

Analysis of gene expression

RNA was isolated from the distal 2 cm of each intestinal segment using Trizol (Invitrogen), followed by DNase treatment using the RNeasy Mini Kit (Qiagen). For intestinal organ cultures, RNA was isolated from segments B and C with the RNeasy Mini Kit. Reverse transcriptase (RT) reactions (50 μl) used 1 μg RNA and the Iscript cDNA Synthesis Kit (Bio-Rad). Quantitative RT-PCR was performed as described (Jain et al., 2006) with SYBR Green dye and the primers listed in supplementary material Table S2. Expression levels were determined with triplicate assays per sample and normalized to the expression of glyceraldehyde-3-phosphate dehydrogenase (*Gapdh*), which remained the same in all samples.

Intestinal organoid culture

Jejunal tissue (~10 cm) was incubated in PBS containing 4 mM EDTA and 1 mM DTT for 30 minutes at 4°C on a rotating platform. After removing villi by light shaking, the tissue was transferred into a tube with PBS. Crypts were released by vigorous shaking then passed through a 70-μm filter (Becton Dickenson). Crypts were quantitated, pelleted (13 ***g***, 7 minutes) and resuspended in 50 μl Matrigel (BD Biosciences) supplemented with 50 ng/ml EGF (R&D Systems), 5 ng/ml WNT3A (R&D Systems), 1 μg/ml R-spondin 1 (R&D Systems) and 100 ng/ml noggin (PeproTech). After polymerization at 37°C for 30 minutes, 0.5 ml culture medium was added to each well and the culture was maintained as described (Gracz et al., 2010).

Twenty-four hours post-plating, organoid cultures were treated with vehicle or 25 μM DAPT daily for 5 days. Four representative organoids from each condition were digitally imaged under bright-field microscopy. Organoid area was measured using ImageJ (NIH, http://imagej.nih.gov/ij/).

For analysis of organoid stem cell activity, isolated crypts were established in culture for 24 hours before daily treatment with vehicle or 25 μM DAPT for 2-5 days, followed by measurement of organoid initiating activity after passaging. Treated organoids were mechanically dissociated by passing both media and Matrigel through a 1-ml pipette tip seven times and a 30-gauge needle four times, split 1:3, and plated in Matrigel as described above with the addition of 1 μM jagged 1 (AnaSpec, San Jose, CA, USA) and without DAPT. Organoids were counted 2 days post-passage.

OLFM4 luciferase constructs and transfection analysis

We used previously described plasmid constructs for human OLFM4 (427OLFM4-luciferase) (Chin et al., 2008), the Notch transcriptional inhibitor dominant-negative mastermind (dnMAML) (MCSV-dnMAML) (Maillard et al., 2004) and the Notch pathway activator 3×Flag-NICD1 (Ong et al., 2006). RBP-Jκ binding sites were identified using the

consensus (C/A/T)(G/A)TG(G/A/T)GAA (Tun et al., 1994). Deletion of the human *OLFM4* promoter sequence used the overlap extension PCR technique with outer primers RVprimer3 (5′-CTAGCAAAAT-AGGCTGTCCC-3′) and GLprimer2 (5′-CTTTATGTTTTTGGC-GTCTTCCA-3′) (Promega, pGL3-basic) and the inner mutant primers listed in supplementary material Table S2. Deletion of RBP-Jκ sites used the QuikChange Mutagenesis Kit (Stratagene/Agilent Technologies) and the primers listed in supplementary material Table S3. All constructs were verified by DNA sequencing.

LS174T human colon cancer cells (ATCC #CL-188) were grown in MEM (Gibco) containing 10% fetal calf serum, sodium pyruvate, non-essential amino acids and Pen-Strep-Glut. Transient transfections used Lipofectamine 2000 (Invitrogen) according to the manufacturer's recommendations. Cell lysates were collected at 24 hours post-transfection and luciferase activity was assayed in triplicate with a PerkinElmer Victor^3 luminometer using 20 µl of cell lysate and Dual Luciferase Reagents (Promega). Luciferase activity was normalized to total protein content as determined using the BCA Protein Assay Kit (Thermo Scientific).

Chromatin immunoprecipitation (ChIP)

LS174T cells were transfected with pCS2 (control) or 3×Flag-NICD1 as described above. ChIP was performed according to published protocols from Upstate Biotech with minor modifications (Patel et al., 2007). Sonication was performed on ice with five 20-second pulses using a microtip probe sonicator (Branson Sonifier 250) with output control set to 2.5. Immunoprecipitation used 15 µg of chromatin and 5 µg antibodies – either rabbit IgG (Jackson ImmunoResearch) or anti-Notch1 (Bethyl Labs, Montgomery, TX, USA), which targets the C-terminus of the Notch1 receptor. The precipitated chromatin was reconstituted in water and qRT-PCR quantification of DNA relative to input was performed in triplicate with the primer sequences listed in supplementary material Table S4.

To ensure that the Notch1 antibody specifically immunoprecipitated FLAG-tagged NICD, 50 µl of supernatant was removed from the ChIP assays after incubation with protein-A beads, then 2 µl 5 M NaCl and 10 µl 6× Laemmli sample buffer were added and heated at 95°C for 5 minutes followed by crosslink reversal for 4 hours at 65°C. A sample (40 µl) was separated by SDS-PAGE and immunoblotting was performed with anti-FLAG antibody as previously described (Patel et al., 2007) (supplementary material Fig. S5).

Statistical analysis

Quantitative data are presented as mean ± s.e.m. The effect of a treatment between similar sample groups was analyzed with Student's *t*-test, whereas the effects of genotype within a treatment group and the effects of various expression constructs on luciferase activity were analyzed by one-way ANOVA followed by Dunnett's post-test; $P<0.05$ was considered significant.

RESULTS

Notch signaling is required for CBC stem cell homeostasis

To determine the importance of Notch signaling for intestinal stem cells, we used the *Lgr5-GFP* mouse strain (Barker et al., 2007) to identify and track CBC stem cells after treatment of adult mice with the global Notch pathway inhibitor DBZ. GFP-positive cells were located at the base of the crypts and commonly observed to be dividing in vehicle-treated controls (Fig. 1A). By contrast, there were fewer GFP-positive cells in DBZ-treated crypts, and the remaining GFP-expressing cells were weakly staining and commonly misshapen (Fig. 1B). This finding was supported by decreased *GFP* mRNA abundance in DBZ-treated intestine (Fig. 1C). Morphometric analysis showed an 86% reduction in GFP-positive crypts (Fig. 1D) and a reduction in the number of GFP-labeled cells in each positive crypt, with an average of 4.1 cells in the controls and 2.1 cells per expressing crypt in DBZ-treated intestine (Fig. 1E). This analysis suggested that inhibition of Notch signaling led to an overall reduction in CBC stem cells.

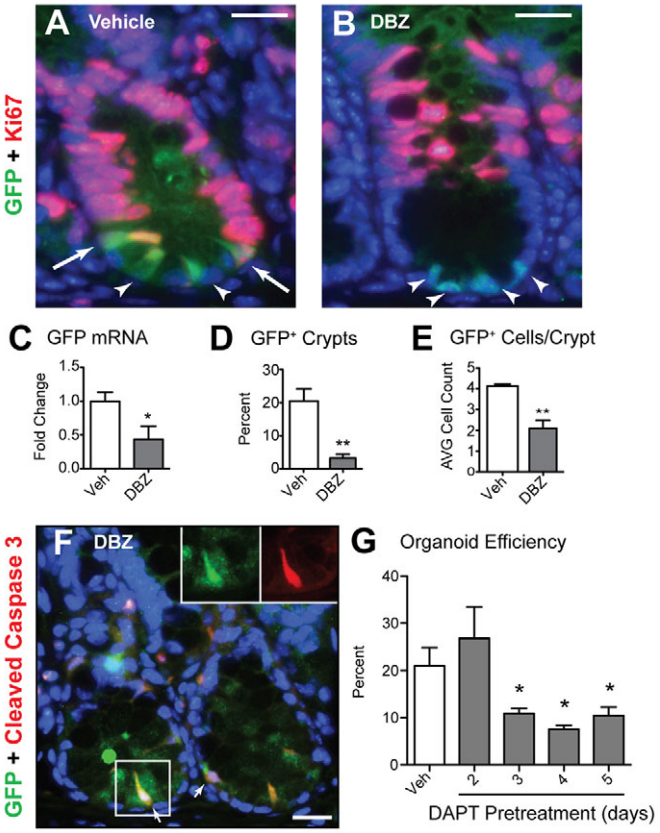

Fig. 1. Loss of crypt base columnar (CBC) stem cells with Notch inhibition. Histological analysis of jejunum from *Lgr5-GFP* mice treated with vehicle (veh) or DBZ (n=4). (**A**,**B**) Co-immunostaining for GFP (green) and Ki67 (red) with DAPI nuclear counterstain (blue). Arrowheads, GFP-positive Ki67-negative cells; arrows, GFP-positive Ki67-positive cells. (**C**) Quantitative reverse transcriptase PCR (qRT-PCR) analysis of *GFP* mRNA abundance. Values were normalized to *Gapdh* expression and are reported as fold-change relative to vehicle control. (**D**,**E**) Morphometric analysis of GFP and Ki67 co-stained paraffin sections, showing the percentage of crypts that contained at least one GFP-positive cell (D) and the average number of GFP-positive cells per expressing crypt (E). (**F**) Co-immunostaining (arrows) for activated caspase 3 (red) and GFP (green). Insets show separate green and red channels of the boxed region. (**G**) Crypts were isolated from adult mice to establish organoids, which were pretreated for 2-5 days with 25 µM DAPT before dispersal and passage to initiate new organoids without further addition of γ-secretase inhibitor (GSI). The efficiency of organoid initiation was assessed 2 days post-passage by calculating the percentage of organoids relative to the initial number of plated crypts. Quantitative data are presented as mean ± s.e.m. *$P<0.05$, **$P<0.01$, by Student's *t*-test compared with vehicle-treated control. Scale bars: 10 µm.

We examined cellular proliferation and apoptotic cell death to determine potential mechanisms for reduced CBC stem cell numbers with Notch inhibition. Co-staining for GFP and Ki67 demonstrated a marked reduction in proliferating CBC stem cells in DBZ-treated intestine, with 59% of GFP-positive cells co-expressing Ki67 in control intestine versus 24% co-stained cells in intestine from DBZ-treated mice (Fig. 1; data not shown). In addition, we detected rare apoptotic CBC stem cells in the DBZ-treated intestine after co-immunostaining for GFP and activated caspase 3 (Fig. 1F). By contrast, caspase-positive CBC cells were not observed in vehicle-treated crypts. Reduced cellular proliferation coupled with cell death

is consistent with the observed decrease in CBC stem cell numbers. The reduction in stem cell number predicts that Notch inhibition would diminish overall stem cell activity. This was tested in crypt organoid cultures. Treatment with the GSI DAPT showed a marked reduction in organoid growth (supplementary material Fig. S1) and subculturing after discontinuation of DAPT demonstrated that Notch inhibition reduced the efficiency of new organoid initiation, consistent with reduced stem cell activity (Fig. 1G). Together, these studies demonstrated that Notch signaling is crucial for the maintenance of intestinal CBC stem cells.

Notch regulates *Olfm4* expression

To confirm that Notch pathway inhibition regulates CBC stem cells, we measured the expression of the marker genes *Olfm4*, *Lgr5* and *Ascl2*. This revealed a striking reduction in *Olfm4* mRNA abundance in DBZ-treated intestine (Fig. 2A), to an extent greater than the decrease in GFP-stained CBC cell number (Fig. 1). Although GSIs appear to principally affect Notch signaling based on the similarity of the phenotypes observed with DBZ treatment and genetic inhibition of the pathway (Milano et al., 2004; van Es et al., 2005; Riccio et al., 2008), it is known that the γ-secretase enzyme complex can cleave other proteins in addition to Notch receptors (Tolia and De Strooper, 2009). Therefore, we used pathway-specific models to confirm Notch regulation of *Olfm4*. Treatment of adult mice with a combination of neutralizing antibodies directed against the Notch1 and Notch2 receptors (Wu et al., 2010) resulted in a marked decrease in *Olfm4* mRNA abundance (Fig. 2B), similar to the effect of DBZ treatment. Conversely, *Olfm4* expression was increased 1.9-fold in the intestines of newborn Vil-Cre; $Rosa^{NotchIC}$ mice (Fig. 2C), which exhibit constitutive activation of Notch signaling throughout the intestinal epithelium (Fre et al., 2005; Stanger et al., 2005). Similar regulation was observed in the human colon cancer cell line LS174T, with endogenous *OLFM4* mRNA abundance markedly decreased after GSI treatment and increased 1.8-fold following activation of Notch signaling by transfection of a Notch1 intracellular domain (NICD1) expression construct (Fig. 2D). Notch responsiveness of *OLFM4* was further confirmed in LS174T cells by decreased expression of a luciferase promoter construct (427OLFM4-luciferase) after DAPT treatment and by increased expression after Notch activation with NICD1 (Fig. 2E). Together, these data show that intestinal *Olfm4* expression is Notch responsive.

Expression of the CBC stem cell markers *Lgr5* and *Ascl2* was also reduced after Notch inhibition, consistent with the observed decreases in CBC stem cell number (Fig. 2A,B), but these decreases were modest in comparison to *Olfm4*. The more modest changes could be due to alteration of other signaling pathways, such as Wnt signaling, which is known to regulate the expression of both *Ascl2* and *Lgr5* (van der Flier et al., 2009). In addition, because *Lgr5* is also expressed in short-lived progenitor cell populations (van der Flier et al., 2009), the overall level of expression might reflect a balance of reduced numbers of CBC stem cells and increased numbers of TA progenitors. Indeed, we observed increased expression of the progenitor cell marker *Prom1* (Snippert et al., 2009; Zhu et al., 2009) in both DBZ-treated and Notch1/2 antibody-treated intestine (Fig. 2A,B), which would be consistent with increased numbers of short-lived progenitors after Notch inhibition.

Inhibition of Notch signaling disturbs intestinal epithelial cell differentiation

Histological analysis demonstrated that the general reduction in cellular proliferation in DBZ-treated intestine (Fig. 1; supplementary material Fig. S1) was coupled with precocious

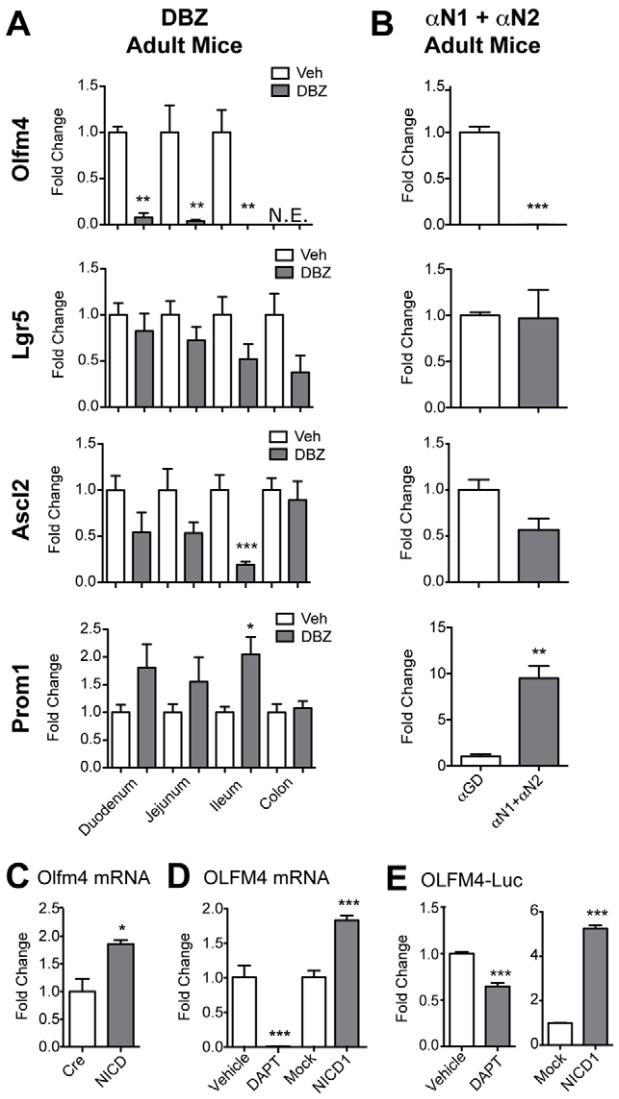

Fig. 2. The CBC stem cell marker *Olfm4* is a sensitive readout of intestinal Notch activity. (**A**,**B**) Stem/progenitor marker expression was determined by qRT-PCR analysis of intestinal RNAs from adult mice treated with vehicle (veh) or DBZ (n=6) (A) or from duodenum treated with neutralizing antibodies against Notch1 and Notch2 (αN1 + αN2) or an isotype control (αGD) (n=3) (B). *Olfm4* is not expressed (N.E.) in the mouse colon. (**C**) *Olfm4* expression levels in newborn Vil-Cre (Cre) and Vil-Cre; $Rosa^{NotchIC}$ (NICD) intestine (n=5). (**D**,**E**) *Olfm4* expression (D) or 427OLFM4-luciferase activity (E) in the human colon cancer cell line LS174T treated with vehicle or DAPT (40 μM) or transfected with empty vector (Mock) or NICD1 (n=3). Gene expression values were normalized to *Gapdh*. Luciferase activity values were normalized to total protein content. All data are expressed as mean ± s.e.m. of the fold-change relative to the corresponding control-treated region/group. *P<0.05, **P<0.01, ***P<0.001.

differentiation of progenitors into secretory cell types (Fig. 3). It is well established that Notch signaling inhibits the differentiation of secretory cells (Fre et al., 2005; Stanger et al., 2005); however, there have been conflicting reports on the specific cellular changes induced by global Notch inhibition. Although all studies have reported goblet cell hyperplasia, the effect of blocking Notch on enteroendocrine and Paneth cells has been disputed (Milano et al., 2004; van Es et al., 2005; Riccio et

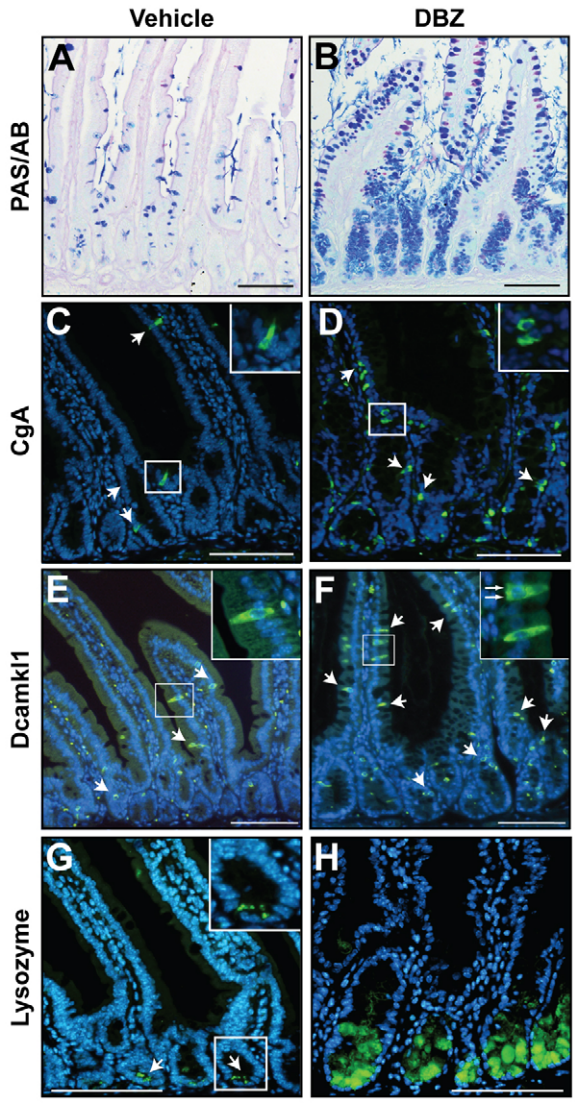

Fig. 3. Notch inhibition leads to secretory cell hyperplasia. Secretory cell populations were analyzed in the duodenum of vehicle-treated (A,C,E,G) and DBZ-treated (B,D,F,H) adult mice. (**A**,**B**) Goblet cells were stained with periodic acid-Schiff/Alcian Blue (PAS/AB). (**C**,**D**) Enteroendocrine cells were identified by immunostaining for chromogranin A (CgA; green, arrows). (**E**,**F**) Tuft cells were identified by DCAMKL1 immunostaining (green, arrows). (**G**,**H**) Paneth cells were identified by lysozyme immunostaining (green). Arrows indicate punctate staining in mature Paneth cells in vehicle-treated intestine. Insets show high-magnification views of the boxed regions. DAPI (blue) was used as nuclear counterstain in C-H. Scale bars: 100 μm.

al., 2008; Kazanjian et al., 2010; Kim and Shivdasani, 2011; Pellegrinet et al., 2011). We examined markers of these different lineages in the DBZ-treated mice. As expected, we observed marked goblet cell hyperplasia with PAS/Alcian Blue staining in DBZ-treated mice (Fig. 3A,B). Importantly, we also observed increased numbers of cells staining for the enteroendocrine marker chromogranin A (Fig. 3C,D), the tuft cell marker DCAMKL1 (Dclk1 – Mouse Genome Informatics) (Fig. 3E,F) (Gerbe et al., 2011; Saqui-Salces et al., 2011) and the Paneth cell marker lysozyme (Fig. 3G,H), suggesting that Notch inhibition expands all secretory cell types and not only goblet cells.

Although there was a robust increase in lysozyme-positive cells in DBZ intestine, the staining pattern was abnormal, with diffuse cytoplasmic staining instead of the normal punctate pattern, suggesting that Paneth cell secretory granules were not properly formed when Notch signaling was inhibited (Fig. 3G,H). Ultrastructural analysis by electron microscopy confirmed the disorganized structure of Paneth cells in the DBZ-treated intestine, with cells at the base of the crypts appearing completely filled with both mucus and small electron-dense granules, instead of the large, electron-dense secretory granules observed in Paneth cells from vehicle-treated mice (Fig. 4A,B). We did not observe any cells with normal Paneth cell morphology (i.e. large electron-dense secretory granules, non-mucus-producing) in DBZ-treated intestine.

The lysozyme immunostaining in the DBZ-treated crypts appeared to overlap with the goblet cell staining (Fig. 3); thus, we co-stained for goblet (Muc2) and Paneth (Mmp7) cell markers to determine whether these cells co-expressed markers of both secretory cell types. Whereas double-positive cells were rare in vehicle-treated intestine, they were numerous in DBZ-treated intestine, where they filled elongated crypts (Fig. 4C,D). These unusual secretory cells were most abundant in the distal small intestine of DBZ-treated mice, although they were observed throughout the intestine, including small clusters of double-positive cells at the base of the colonic crypts (Fig. 4E,F). The double-positive cells also expressed Sox9, a transcription factor that is normally highly expressed in mature Paneth cells (Fig. 4G,H) (Bastide et al., 2007; Mori-Akiyama et al., 2007). Moreover, DBZ induced a general increase in the expression of cryptdins, lysozyme and ephrins, suggesting that these unusual secretory cells have initiated the Paneth cell developmental program (supplementary material Fig. S2). The expansion of double-staining cells in DBZ-treated mice suggests that Notch signaling is required to maintain the mature Paneth cell phenotype and that loss of Notch signaling stimulated the formation and accumulation of Sox9-expressing precursors co-expressing Paneth and goblet cell markers. However, because Paneth cells are not thought to directly receive Notch signals, but rather to express Notch ligands (Sato et al., 2011) and Atoh1 (Pinto et al., 2003), this is likely to be a non-cell-autonomous role of Notch signaling. Interestingly, Muc2 expression did not colocalize with the endocrine cell marker chromogranin A (supplementary material Fig. S2), demonstrating that this phenotype did not extend to all secretory cell types.

Notch regulation of *Olfm4* expression is *Atoh1* independent

Consistent with the increase in secretory cells, we observed increased expression of the Notch-regulated transcription factor *Atoh1* in DBZ-treated intestine (Fig. 5A-C). We also observed increased expression of transcription factors that function downstream of *Atoh1* to orchestrate secretory cell differentiation, including *Gfi1* (Shroyer et al., 2005; Bjerknes and Cheng, 2010), *Spdef* (Gregorieff et al., 2009; Noah et al., 2010) and *Neurog3* (Jenny et al., 2002; Bjerknes and Cheng, 2006; Lopez-Diaz et al., 2006) (Fig. 5D-F). Because *Atoh1* has been proposed to mediate intestinal Notch effects, we tested whether Notch regulation of *Olfm4* expression was *Atoh1* dependent. We used the *Atoh1*$^{lacZ/lacZ}$ null mouse (Yang et al., 2001) and a fetal intestine organ culture system for this analysis due to the perinatal lethality of this mutant. Wild-type and *Atoh1* null fetal intestines were cultured, and Notch signaling was inhibited by treatment with GSI. Similar to adult intestine, we observed that Notch inhibition induced a general secretory cell hyperplasia in wild-type intestine, with increased

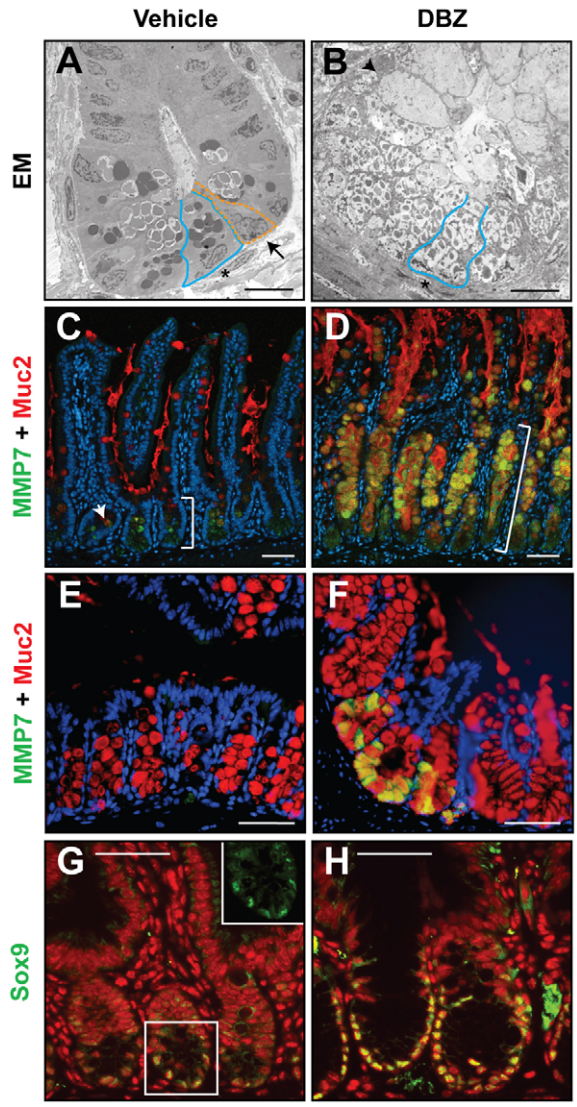

Fig. 4. Accumulation of cells co-expressing Paneth and goblet cell markers with Notch inhibition. Intestines from vehicle-treated (A,C,E,G) and DBZ-treated (B,D,F,H) mice were analyzed for Paneth cell morphology and marker expression. (**A**,**B**) Electron microscopy analysis of jejunal sections. Blue outline (asterisk) marks 'Paneth' cells; orange outline (arrow) marks a CBC stem cell; arrowhead marks a goblet cell. (**C-F**) Co-immunostaining of paraffin sections from ileum (C,D) and colon (E,F) for the Paneth cell marker Mmp7 (green) and the goblet cell marker Muc2 (red) with DAPI nuclear stain (blue) to identify double-positive cells. Crypt height is indicated with brackets in C,D. Rare double-positive cells were observed in vehicle-treated control ileum (C, arrowhead). (**G**,**H**) Immunostaining jejunum for the transcription factor Sox9 (green) with DAPI nuclear stain (pseudo-colored red). Inset shows green channel of the boxed area. Scale bars: 10 μm in A,B; 50 μm in C-H.

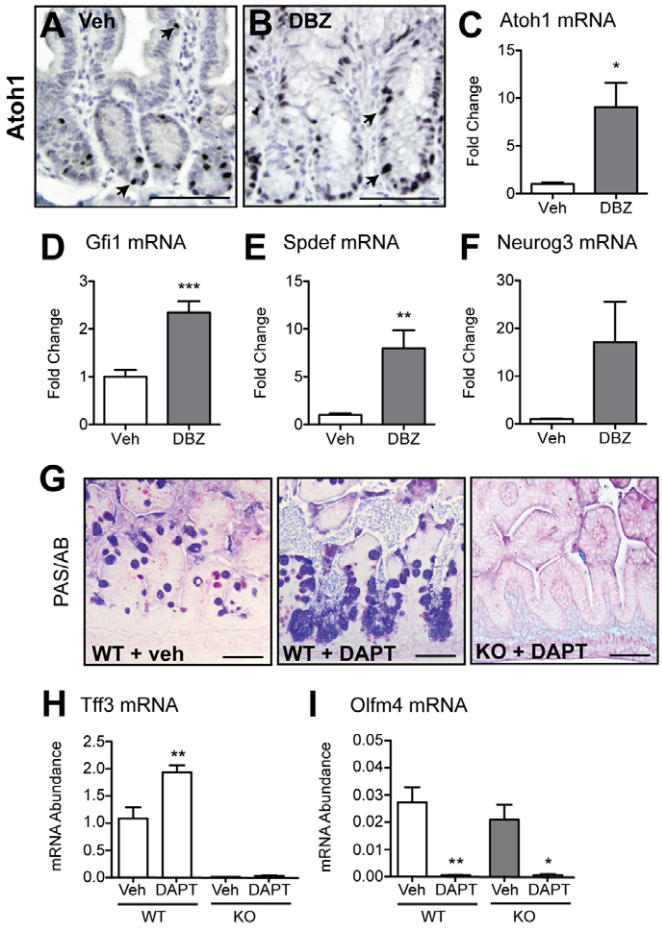

Fig. 5. Notch regulation of *Olfm4* expression is *Atoh1* independent. (**A**,**B**) Immunostaining of duodenum for Atoh1-positive cells (brown, arrowheads) in vehicle (veh)- and DBZ-treated mice. (**C-F**) Expression of the indicated transcription factors was determined by qRT-PCR analysis of duodenal RNAs from mice treated with vehicle or DBZ. Values were normalized to *Gapdh* and are expressed as fold-change relative to the vehicle control. n=4; *P<0.05, **P<0.01, ***P<0.001. (**G-I**) Analysis of fetal intestine cultured from wild-type (WT) and *Atoh1*$^{lacZ/lacZ}$ (KO) mice treated with vehicle or 40 μM DAPT for 3 days. (G) Goblet cells were visualized by PAS/AB. (H,I) Expression of the goblet cell marker *Tff3* (H) and the CBC marker *Olfm4* (I) was determined by qRT-PCR. Values were normalized to *Gapdh* and are presented as the mean ± s.e.m. n=3-6, *P<0.05, **P<0.01, compared with vehicle treatment of the same genotype. Scale bars: 50 μm.

staining for goblet, enteroendocrine and Paneth cells (Fig. 5G; supplementary material Fig. S3). Increased lysozyme staining was particularly interesting because Paneth cells do not normally mature until after birth (Cheng, 1974). Similar to adult intestine, these lysozyme-positive cells co-stained for goblet cell markers (not shown). Consistent with previously published studies (Kazanjian et al., 2010; van Es et al., 2010; Kim and Shivdasani, 2011), we observed that increased secretory cell differentiation following Notch inhibition was completely dependent on *Atoh1*; goblet cells and markers were not detected in DAPT-treated *Atoh1* null intestine (Fig. 5G,H), nor were enteroendocrine or Paneth cell markers (supplementary material Fig. S4). Interestingly, *Atoh1*$^{lacZ/-}$ intestine expressed intermediate levels of *Atoh1* as well as its downstream effectors *Gfi1*, *Spdef* and *Neurog3* (supplementary material Fig. S4).

In contrast to the effects on cell fate, *Olfm4* expression was similarly downregulated in null and wild-type intestine after DAPT treatment, demonstrating that Notch regulation of this CBC stem cell marker is *Atoh1* independent (Fig. 5I). Our finding differs from a previous study in adult Atoh1-deficient intestine, which reported that *Olfm4* was not affected by DBZ treatment in this mutant (van Es et al., 2010). This discrepancy is likely to be explained by

differences between the two studies in the timing of analysis after DBZ administration. In contrast to our protocol in which expression was measured 1 day after GSI treatment, the van Es et al. study used a 7-day chase period, which might allow *Olfm4* expression to return to baseline. Accordingly, we have observed that *Olfm4* expression returns to baseline 3 days after a single injection of DBZ (A.J.C. and L.C.S., unpublished), suggesting that Notch regulation of this CBC gene is rapid and dynamic. Furthermore, analysis of Notch regulation of *Olfm4* in the fetal organ culture system revealed that expression was decreased within 1 day of Notch inhibition and with low doses of DAPT (supplementary material Fig. S4). Together, our studies showed that *Atoh1* is required for Notch regulation of cell fate, but is not required for Notch regulation of *Olfm4* expression in CBC stem cells.

Olfm4 is a direct Notch target gene

Our finding that Notch is required for *Olfm4* expression in CBC stem cells suggested that Notch signaling directly targets this gene. Several RBP-Jκ consensus sites were identified in the human and mouse genes, including three sites in the 427 bp human *OLFM4* promoter (Fig. 6A; data not shown). Deletion of regions that contained each of the sites in the proximal promoter region mapped the critical activity to a 90 bp region containing the RBPJκ-a site and an E-box consensus site. Further analysis of constructs containing targeted mutations confirmed that the RBPJκ-a site (ΔRBPJκ-a), and not the E-box or the RBPJκ-b sites, was required for Notch responsiveness of this luciferase construct (Fig. 6C; data not shown). Moreover, co-transfection with the canonical Notch inhibitor dnMAML resulted in attenuated activity of the 427OLFM4-luciferase construct and further lowered the basal luciferase activity of ΔRBPJκ-a (Fig. 6C). This study demonstrated that *OLFM4* transcription is regulated by canonical Notch signaling through consensus RBP-Jκ binding sites.

We next used ChIP analysis to test whether NICD directly binds to the *OLFM4* promoter. Occupation of the proximal *OLFM4* promoter increased 3.7-fold in the presence of constitutive Notch signaling (Fig. 6D). Similar results were obtained for other *OLFM4* gene segments containing RBP-Jκ consensus sites further upstream and in the first intron (supplementary material Fig. S5) and for a region of the *HES1* gene that contains active RBP-Jκ binding sites (Arnett et al., 2010) (Fig. 6E). By contrast, increased NICD occupation was not observed at a distant upstream site in the *OLFM4* promoter region (Fig. 6D). Together, these data show that *OLFM4* is a direct transcriptional target of canonical Notch signaling. Furthermore, because this gene is specifically expressed in the CBC stem cell, these results demonstrate that Notch signaling directly regulates this cell. To our knowledge, this is the first direct cellular target of Notch signaling identified in the intestine.

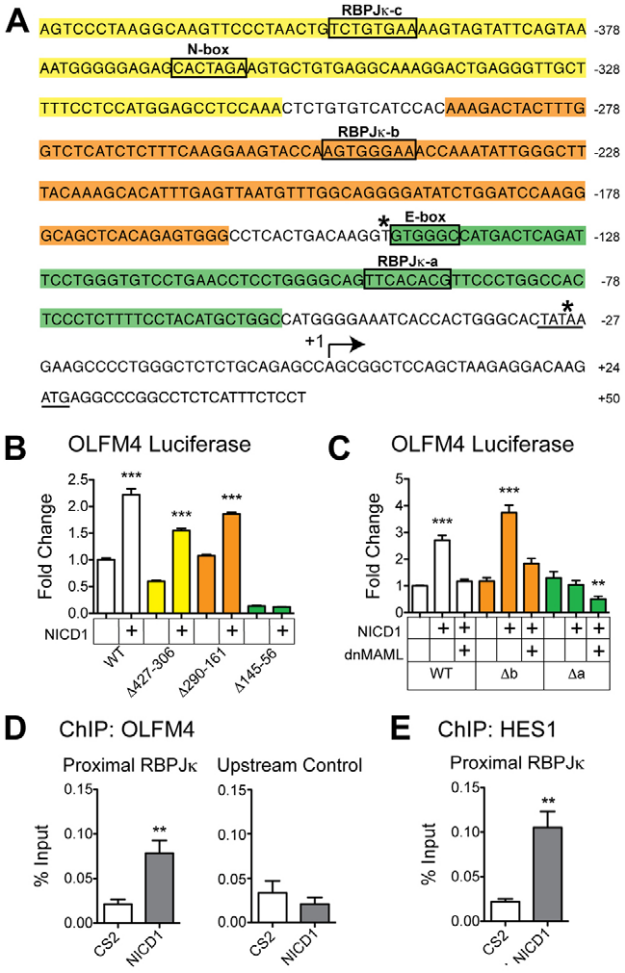

Fig. 6. *OLFM4* transcription is regulated by canonical Notch signaling. (**A**) The proximal promoter sequence of the human *OLFM4* gene, featuring three RBP-Jκ consensus binding sites, an N-box, an E-box, the TATA box (underlined), transcription start site (arrow, +1) and translation start site (underlined). The asterisks at –146 and –28 indicate the positions of primers used to amplify chromatin in the immunoprecipitation (ChIP) analysis. (**B**,**C**) Luciferase activity was measured in LS174T cells that were co-transfected with the full-length human 427OLFM4-luciferase construct (WT) or mutant OLFM4 luciferase constructs (Δ427-306, Δ290-161 or Δ145-56) together with either empty vector or the NICD1 expression construct (B). Mutant constructs with targeted deletions of the RBPJκ-b (Δb) or RBPJκ-a (Δa) consensus sites were transfected with NICD1, dominant-negative mastermind (dnMAML), or both (C). Bar colors correspond to the shaded sequence regions in A that were altered in each mutant construct. Transfection data are reported as fold-change relative to untreated WT controls. n=3 experiments performed in triplicate; $^{**}P<0.01$, $^{***}P<0.001$. (**D**) ChIP of the proximal region containing RBP-Jκ sites or of a distant upstream region without RBP-Jκ sites was performed in LS174T cells transfected with either vector control (CS2) or NICD1. (**E**) ChIP of a *HES1* promoter region that contains known RBP-Jκ consensus sites. ChIP data were normalized by subtracting the values of the control IgG samples from those of the Notch antibody samples and are presented as the percentage of the initial chromatin input. n=4 independent experiments, qPCR performed in triplicate; $^{**}P<0.01$. Values are presented as the mean ± s.e.m.

DISCUSSION

We demonstrate in this study that active Notch signaling is required for the maintenance of CBC stem cells in the small intestine. Notch inhibition resulted in stem cell loss, with both decreased proliferation and apoptotic cell death contributing to the overall reduction in CBC stem cell number. Notch inhibition also reduced the efficiency of organoid initiation, demonstrating a requirement of Notch for stem cell function. Consistent with stem cell loss was the observation that loss of Notch signaling was irreparable, with death occurring 3 days following a 5-day GSI treatment course (data not shown). Our demonstration that Notch signaling is essential for survival of the mouse CBC stem cell differs from recent studies in *Drosophila* showing increased proliferation of midgut stem cells with loss of Notch (Takashima et al., 2011),

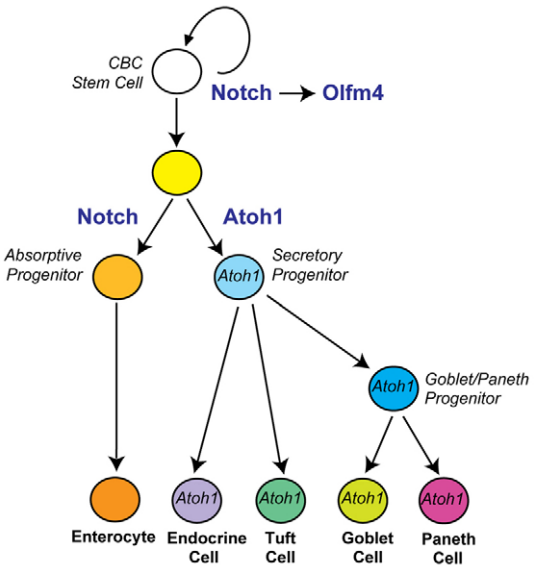

Fig. 7. Notch signaling regulates several aspects of intestinal epithelial cell homeostasis. A summary of the major findings of this study, showing that Notch regulates multiple aspects of intestinal epithelial cell differentiation. (1) Notch signaling directly targets the CBC stem cell to activate *Olfm4* transcription, maintain proliferation and promote cell survival. (2) Notch acts to promote differentiation to the absorptive lineage by repressing *Atoh1* transcription. Although the specific cellular target for this function has not been identified, Notch is likely to act on a transit-amplifying progenitor cell to bias cell fate choice to absorptive rather than secretory cells. (3) Notch appears to act later, in an indirect manner, to segregate the Paneth/goblet cell lineage and/or maintain the mature Paneth cell phenotype.

suggesting fundamental differences between fly and mammalian intestinal stem cells.

We observed a rapid and substantial reduction of *Olfm4* mRNA in both adult and fetal intestine after Notch inhibition and increased *Olfm4* expression after constitutive activation of Notch signaling. We demonstrated that the mechanism of human *OLFM4* gene regulation was transcriptional, with promoter activity directly regulated through NICD binding to canonical RBP-Jκ consensus binding sites. This finding confirmed that Notch directly targets the CBC stem cell and establishes *Olfm4* as a sensitive transcriptional readout of Notch signaling in the intestine. In contrast to *Olfm4*, expression of the other CBC marker genes, *Lgr5* and *Ascl2*, was not affected by Notch inhibition, with continued expression perhaps reflecting their regulation by Wnt signaling (van der Flier et al., 2009).

Currently, the intestinal function of Olfm4 protein is unknown; however, studies in other tissues have suggested that Olfm4 has functions associated with stem cell properties. Murine Olfm4 was originally identified in hematopoietic precursor cells (Zhang et al., 2002) and has since been characterized as a secreted extracellular matrix glycoprotein that can facilitate cell adhesion and bind to cell surface cadherins and lectins (Liu et al., 2006). It is a member of a family of olfactomedin domain-containing proteins that have been suggested to function in wide-ranging cellular activities, such as cell adhesion, cell cycle regulation and tissue patterning, and have been proposed to modulate Wnt and BMP signaling (Tomarev and Nakaya, 2009). Although studies have suggested that Olfm4 regulates proliferation and apoptosis (Zhang et al., 2004; Kobayashi et al., 2007), which are processes relevant for stem cell function, the intestinal function of Olfm4 remains obscure. A recent study of Olfm4-deficient mice showed normal intestinal histology, demonstrating that this protein is not required for intestine development (Liu et al., 2010); however, intestinal stem cell function was not critically analyzed in this study. Because other olfactomedin family members are expressed in intestine (data not shown), compensatory pathways could mask the role of Olfm4 in this mutant mouse.

Our findings suggest that Notch signaling regulates multiple aspects of intestinal epithelial cell homeostasis. In addition to loss of CBC stem cells, disruption of Notch signaling had profound effects on progenitor cell proliferation and cell fate determination, including a likely non-cell-autonomous effect on the terminal differentiation and maintenance of Paneth cells. A model that depicts these different aspects of Notch regulation in the intestine is shown in Fig. 7. We observed that Notch inhibition stimulated precocious differentiation of progenitors into cells of the secretory lineage, including goblet cells, endocrine cells, tuft cells and cells co-expressing goblet (Muc2) and Paneth (lysozyme and Mmp7) cell markers. The accumulation of cells double-positive for goblet and Paneth cell markers in the crypts of DBZ-treated mice had not been previously reported. Although this phenotype was most apparent in the distal small intestine, where the DBZ-treated crypts were filled with double-positive cells, they were also observed in other regions, including the colon and immature intestine, which do not normally contain Paneth cells.

Co-expression of goblet and Paneth cell markers is a feature of ‘intermediate cells’, a rare epithelial cell type that has been proposed to be a precursor for the goblet/Paneth cell lineages (Troughton and Trier, 1969; Garabedian et al., 1997). Interestingly, we observed that many of the double-positive cells induced by Notch inhibition also expressed Prom1 (data not shown), which has been described as a progenitor cell marker in the intestine (Snippert et al., 2009; Zhu et al., 2009). Thus, a portion of the double-positive cells could represent precursors to the goblet/Paneth lineage that have incompletely segregated. However, ultrastructural analysis did not reveal any normal Paneth cells with properly formed secretory granules in DBZ-treated intestine, suggesting that Notch signaling might act to maintain function and to suppress mucin gene expression in mature Paneth cells by an indirect mechanism. Thus, although the mechanism is unclear, our data suggest that Notch signaling plays a crucial role in the segregation of the goblet/Paneth cell lineages and in the terminal differentiation and/or maintenance of the mature Paneth cell phenotype.

Previous studies had demonstrated the central role of Notch signaling for regulating cell fate choice between absorptive and secretory lineages through control of the transcription factor Atoh1 (Yang et al., 2001; Shroyer et al., 2007; VanDussen and Samuelson, 2010). Notch signaling functions to repress Atoh1 expression and thereby guide differentiation to absorptive enterocytes. The singular function of Notch signaling in this decision appears to be *Atoh1* repression because Notch is not required for progenitor cell differentiation into absorptive enterocytes when *Atoh1* is removed (Kim and Shivdasani, 2011). There is some controversy as to whether Notch inhibition results in only goblet cell hyperplasia (van Es et al., 2005; Riccio et al., 2008; Pellegrinet et al., 2011) or the full program of secretory cell activation (Milano et al., 2004; Kazanjian et al., 2010; Kim and Shivdasani, 2011). Our study demonstrates that inhibiting Notch signaling in both immature and adult intestine leads to a robust increase in *Atoh1* expression and to the induction of all four secretory cell lineages and not just goblet

cell hyperplasia. Furthermore, similar to other recent studies (Kazanjian et al., 2010; van Es et al., 2010; Kim and Shivdasani, 2011), we show that *Atoh1* expression is required for increased secretory cell differentiation, as GSI treatment was unable to induce secretory cell differentiation in *Atoh1*-deficient intestine. By contrast, we observed that Notch regulation of *Olfm4* expression was *Atoh1* independent.

In summary, we have shown that Notch signaling is required for CBC stem cell homeostasis. Blocking Notch resulted in fewer stem cells due to reduced proliferation, increased differentiation and apoptotic cell loss. Importantly, we identified the CBC stem cell-specific marker *Olfm4* as a direct Notch target gene. Furthermore, we have shown that the generalized secretory cell hyperplasia induced by Notch inhibition is characterized by the loss of the mature Paneth cell morphology. A recent study suggested that Paneth cells might provide essential niche signals for the CBC stem cells, including the Wnt ligand Wnt3, the Notch ligand Dll4, EGF and TGFα (Sato et al., 2011). Perhaps the morphological changes that we observed in Paneth cells after Notch inhibition could result in the alteration of important niche signals required for normal CBC stem cell homeostasis.

The fundamental importance of Notch for the intestine underscores the challenge of targeting this pathway for treatment of human cancer and other diseases, including Alzheimer's disease (Pannuti et al., 2010). The acute and potentially lethal intestinal toxicity observed with global Notch disruption is a serious obstacle to overcome in the design of drugs that target this pathway. Thus, developing targeted therapies that preserve Notch function in the intestine will be an important future goal.

Acknowledgements

We thank Dr S. Robine for providing Vil-Cre mice; Dr N. Shroyer for *Atoh1*$^{lacZ/lacZ}$ mice; Dr H. Crawford for the rat anti-Mmp7 antibody; Dr G. Rodgers for the 427OLFM4-luciferase construct; Dr R. Kopan for the 3×Flag-NICD1 construct; and B. Nelson for technical assistance with electron microscopy.

Funding

K.L.V. was supported by an American Gastroenterological Association Foundation Graduate Student Fellowship and a Rackham Predoctoral Fellowship. The research was funded by the National Institutes of Health [RO1-DK56882, RO1-DK78927 to L.C.S.] and the Cell Biology and Imaging Core of the Michigan Gastrointestinal Peptide Center [P30 DK34933]. Deposited in PMC for release after 12 months.

Competing interests statement

The authors declare no competing financial interests.

Supplementary material

Supplementary material available online at
http://dev.biologists.org/lookup/suppl/doi:10.1242/dev.070763/-/DC1

References

Arnett, K. L., Hass, M., McArthur, D. G., Ilagan, M. X., Aster, J. C., Kopan, R. and Blacklow, S. C. (2010). Structural and mechanistic insights into cooperative assembly of dimeric Notch transcription complexes. *Nat. Struct. Mol. Biol.* **17**, 1312-1317.

Barker, N., van Es, J. H., Kuipers, J., Kujala, P., van den Born, M., Cozijnsen, M., Haegebarth, A., Korving, J., Begthel, H., Peters, P. J. et al. (2007). Identification of stem cells in small intestine and colon by marker gene Lgr5. *Nature* **449**, 1003-1007.

Bastide, P., Darido, C., Pannequin, J., Kist, R., Robine, S., Marty-Double, C., Bibeau, F., Scherer, G., Joubert, D., Hollande, F. et al. (2007). Sox9 regulates cell proliferation and is required for Paneth cell differentiation in the intestinal epithelium. *J. Cell Biol.* **178**, 635-648.

Benedito, R. and Duarte, A. (2005). Expression of Dll4 during mouse embryogenesis suggests multiple developmental roles. *Gene Expr. Patterns* **5**, 750-755.

Bjerknes, M. and Cheng, H. (2006). Neurogenin 3 and the enteroendocrine cell lineage in the adult mouse small intestinal epithelium. *Dev. Biol.* **300**, 722-735.

Bjerknes, M. and Cheng, H. (2010). Cell Lineage metastability in Gfi1-deficient mouse intestinal epithelium. *Dev. Biol.* **345**, 49-63.

Cheng, H. (1974). Origin, differentiation and renewal of the four main epithelial cell types in the mouse small intestine. IV. Paneth cells. *Am. J. Anat.* **141**, 521-535.

Cheng, H. and Leblond, C. P. (1974a). Origin, differentiation and renewal of the four main epithelial cell types in the mouse small intestine. I. Columnar cell. *Am. J. Anat.* **141**, 461-479.

Cheng, H. and Leblond, C. P. (1974b). Origin, differentiation and renewal of the four main epithelial cell types in the mouse small intestine. V. Unitarian theory of the origin of the four epithelial cell types. *Am. J. Anat.* **141**, 537-561.

Chin, K. L., Aerbajinai, W., Zhu, J., Drew, L., Chen, L., Liu, W. and Rodgers, G. P. (2008). The regulation of OLFM4 expression in myeloid precursor cells relies on NF-kappaB transcription factor. *Br. J. Haematol.* **143**, 421-432.

Crosnier, C., Vargesson, N., Gschmeissner, S., Ariza-McNaughton, L., Morrison, A. and Lewis, J. (2005). Delta-Notch signalling controls commitment to a secretory fate in the zebrafish intestine. *Development* **132**, 1093-1104.

Fingleton, B., Powell, W. C., Crawford, H. C., Couchman, J. R. and Matrisian, L. M. (2007). A rat monoclonal antibody that recognizes pro- and active MMP-7 indicates polarized expression in vivo. *Hybridoma (Larchmt)* **26**, 22-27.

Fre, S., Huyghe, M., Mourikis, P., Robine, S., Louvard, D. and Artavanis-Tsakonas, S. (2005). Notch signals control the fate of immature progenitor cells in the intestine. *Nature* **435**, 964-968.

Garabedian, E. M., Roberts, L. J., McNevin, M. S. and Gordon, J. I. (1997). Examining the role of Paneth cells in the small intestine by lineage ablation in transgenic mice. *J. Biol. Chem.* **272**, 23729-23740.

Gerbe, F., van Es, J. H., Makrini, L., Brulin, B., Mellitzer, G., Robine, S., Romagnolo, B., Shroyer, N. F., Bourgaux, J. F., Pignodel, C. et al. (2011). Distinct ATOH1 and Neurog3 requirements define tuft cells as a new secretory cell type in the intestinal epithelium. *J. Cell Biol.* **192**, 767-780.

Gracz, A. D., Ramalingam, S. and Magness, S. T. (2010). Sox9 expression marks a subset of CD24-expressing small intestine epithelial stem cells that form organoids in vitro. *Am. J. Physiol. Gastrointest. Liver Physiol.* **298**, G590-G600.

Gregorieff, A., Stange, D. E., Kujala, P., Begthel, H., van den Born, M., Korving, J., Peters, P. J. and Clevers, H. (2009). The ets-domain transcription factor Spdef promotes maturation of goblet and paneth cells in the intestinal epithelium. *Gastroenterology* **137**, 1333-1345.

Jain, R. N., Brunkan, C. S., Chew, C. S. and Samuelson, L. C. (2006). Gene expression profiling of gastrin target genes in parietal cells. *Physiol. Genomics* **24**, 124-132.

Jenny, M., Uhl, C., Roche, C., Duluc, I., Guillermin, V., Guillemot, F., Jensen, J., Kedinger, M. and Gradwohl, G. (2002). Neurogenin3 is differentially required for endocrine cell fate specification in the intestinal and gastric epithelium. *EMBO J.* **21**, 6338-6347.

Jensen, J., Pedersen, E. E., Galante, P., Hald, J., Heller, R. S., Ishibashi, M., Kageyama, R., Guillemot, F., Serup, P. and Madsen, O. D. (2000). Control of endodermal endocrine development by Hes-1. *Nat. Genet.* **24**, 36-44.

Kazanjian, A., Noah, T., Brown, D., Burkart, J. and Shroyer, N. F. (2010). Atonal homolog 1 is required for growth and differentiation effects of notch/gamma-secretase inhibitors on normal and cancerous intestinal epithelial cells. *Gastroenterology* **139**, 918-928.

Keeley, T. M. and Samuelson, L. C. (2010). Cytodifferentiation of the postnatal mouse stomach in normal and Huntingtin-interacting protein 1-related-deficient mice. *Am. J. Physiol. Gastrointest. Liver Physiol.* **299**, G1241-G1251.

Kim, T. H. and Shivdasani, R. A. (2011). Genetic evidence that intestinal notch functions vary regionally and operate through a common mechanism of Math1 repression. *J. Biol. Chem.* **286**, 11427-11433.

Kobayashi, D., Koshida, S., Moriai, R., Tsuji, N. and Watanabe, N. (2007). Olfactomedin 4 promotes S-phase transition in proliferation of pancreatic cancer cells. *Cancer Sci.* **98**, 334-340.

Liu, W., Chen, L., Zhu, J. and Rodgers, G. P. (2006). The glycoprotein hGC-1 binds to cadherin and lectins. *Exp. Cell Res.* **312**, 1785-1797.

Liu, W., Yan, M., Liu, Y., Wang, R., Li, C., Deng, C., Singh, A., Coleman, W. G., Jr and Rodgers, G. P. (2010). Olfactomedin 4 down-regulates innate immunity against Helicobacter pylori infection. *Proc. Natl. Acad. Sci. USA* **107**, 11056-11061.

Lopez-Diaz, L., Hinkle, K. L., Jain, R. N., Zavros, Y., Brunkan, C. S., Keeley, T., Eaton, K. A., Merchant, J. L., Chew, C. S. and Samuelson, L. C. (2006). Parietal cell hyperstimulation and autoimmune gastritis in cholera toxin transgenic mice. *Am. J. Physiol. Gastrointest. Liver Physiol.* **290**, G970-G979.

Maillard, I., Weng, A. P., Carpenter, A. C., Rodriguez, C. G., Sai, H., Xu, L., Allman, D., Aster, J. C. and Pear, W. S. (2004). Mastermind critically regulates Notch-mediated lymphoid cell fate decisions. *Blood* **104**, 1696-1702.

Milano, J., McKay, J., Dagenais, C., Foster-Brown, L., Pognan, F., Gadient, R., Jacobs, R. T., Zacco, A., Greenberg, B. and Ciaccio, P. J. (2004). Modulation of notch processing by gamma-secretase inhibitors causes intestinal goblet cell metaplasia and induction of genes known to specify gut secretory lineage differentiation. *Toxicol. Sci.* **82**, 341-358.

Mori-Akiyama, Y., van den Born, M., van Es, J. H., Hamilton, S. R., Adams, H. P., Zhang, J., Clevers, H. and de Crombrugghe, B. (2007). SOX9 is required for the differentiation of paneth cells in the intestinal epithelium. *Gastroenterology* **133**, 539-546.

Murtaugh, L. C., Stanger, B. Z., Kwan, K. M. and Melton, D. A. (2003). Notch signaling controls multiple steps of pancreatic differentiation. *Proc. Natl. Acad. Sci. USA* **100**, 14920-14925.

Noah, T. K., Kazanjian, A., Whitsett, J. and Shroyer, N. F. (2010). SAM pointed domain ETS factor (SPDEF) regulates terminal differentiation and maturation of intestinal goblet cells. *Exp. Cell Res.* **316**, 452-465.

Ong, C. T., Cheng, H. T., Chang, L. W., Ohtsuka, T., Kageyama, R., Stormo, G. D. and Kopan, R. (2006). Target selectivity of vertebrate notch proteins. Collaboration between discrete domains and CSL-binding site architecture determines activation probability. *J. Biol. Chem.* **281**, 5106-5119.

Pannuti, A., Foreman, K., Rizzo, P., Osipo, C., Golde, T., Osborne, B. and Miele, L. (2010). Targeting Notch to target cancer stem cells. *Clin. Cancer Res.* **16**, 3141-3152.

Patel, S. R., Kim, D., Levitan, I. and Dressler, G. R. (2007). The BRCT-domain containing protein PTIP links PAX2 to a histone H3, lysine 4 methyltransferase complex. *Dev. Cell* **13**, 580-592.

Pellegrinet, L., Rodilla, V., Liu, Z., Chen, S., Koch, U., Espinosa, L., Kaestner, K. H., Kopan, R., Lewis, J. and Radtke, F. (2011). Dll1- and Dll4-mediated Notch signaling are required for homeostasis of intestinal stem cells. *Gastroenterology* **140**, 1230-1240.

Pinto, D., Robine, S., Jaisser, F., El Marjou, F. E. and Louvard, D. (1999). Regulatory sequences of the mouse villin gene that efficiently drive transgenic expression in immature and differentiated epithelial cells of small and large intestines. *J. Biol. Chem.* **274**, 6476-6482.

Pinto, D., Gregorieff, A., Begthel, H. and Clevers, H. (2003). Canonical Wnt signals are essential for homeostasis of the intestinal epithelium. *Genes Dev.* **17**, 1709-1713.

Riccio, O., van Gijn, M. E., Bezdek, A. C., Pellegrinet, L., van Es, J. H., Zimber-Strobl, U., Strobl, L. J., Honjo, T., Clevers, H. and Radtke, F. (2008). Loss of intestinal crypt progenitor cells owing to inactivation of both Notch1 and Notch2 is accompanied by derepression of CDK inhibitors p27Kip1 and p57Kip2. *EMBO Rep.* **9**, 377-383.

Saqui-Salces, M., Keeley, T. M., Grosse, A. S., Qiao, X. T., El-Zaatari, M., Gumucio, D. L., Samuelson, L. C. and Merchant, J. L. (2011). Gastric tuft cells express DCLK1 and are expanded in hyperplasia. *Histochem. Cell Biol.* **136**, 191-204.

Sato, T., van Es, J. H., Snippert, H. J., Stange, D. E., Vries, R. G., van den Born, M., Barker, N., Shroyer, N. F., van de Wetering, M. and Clevers, H. (2011). Paneth cells constitute the niche for Lgr5 stem cells in intestinal crypts. *Nature* **469**, 415-418.

Schroder, N. and Gossler, A. (2002). Expression of Notch pathway components in fetal and adult mouse small intestine. *Gene Expr. Patterns* **2**, 247-250.

Shroyer, N. F., Wallis, D., Venken, K. J., Bellen, H. J. and Zoghbi, H. Y. (2005). Gfi1 functions downstream of Math1 to control intestinal secretory cell subtype allocation and differentiation. *Genes Dev.* **19**, 2412-2417.

Shroyer, N. F., Helmrath, M. A., Wang, V. Y., Antalffy, B., Henning, S. J. and Zoghbi, H. Y. (2007). Intestine-specific ablation of mouse atonal homolog 1 (Math1) reveals a role in cellular homeostasis. *Gastroenterology* **132**, 2478-2488.

Snippert, H. J., van Es, J. H., van den Born, M., Begthel, H., Stange, D. E., Barker, N. and Clevers, H. (2009). Prominin-1/CD133 marks stem cells and early progenitors in mouse small intestine. *Gastroenterology* **136**, 2187-2194.

Snippert, H. J., van der Flier, L. G., Sato, T., van Es, J. H., van den Born, M., Kroon-Veenboer, C., Barker, N., Klein, A. M., van Rheenen, J., Simons, B. D. et al. (2010). Intestinal crypt homeostasis results from neutral competition between symmetrically dividing Lgr5 stem cells. *Cell* **143**, 134-144.

Stanger, B. Z., Datar, R., Murtaugh, L. C. and Melton, D. A. (2005). Direct regulation of intestinal fate by Notch. *Proc. Natl. Acad. Sci. USA* **102**, 12443-12448.

Takashima, S., Adams, K. L., Ortiz, P. A., Ying, C. T., Moridzadeh, R., Younossi-Hartenstein, A. and Hartenstein, V. (2011). Development of the Drosophila entero-endocrine lineage and its specification by the Notch signaling pathway. *Dev. Biol.* **353**, 161-172.

Tolia, A. and De Strooper, B. (2009). Structure and function of gamma-secretase. *Semin. Cell Dev. Biol.* **20**, 211-218.

Tomarev, S. I. and Nakaya, N. (2009). Olfactomedin domain-containing proteins: possible mechanisms of action and functions in normal development and pathology. *Mol. Neurobiol.* **40**, 122-138.

Troughton, W. D. and Trier, J. S. (1969). Paneth and goblet cell renewal in mouse duodenal crypts. *J. Cell Biol.* **41**, 251-268.

Tun, T., Hamaguchi, Y., Matsunami, N., Furukawa, T., Honjo, T. and Kawaichi, M. (1994). Recognition sequence of a highly conserved DNA binding protein RBP-J kappa. *Nucleic Acids Res.* **22**, 965-971.

van der Flier, L. G., van Gijn, M. E., Hatzis, P., Kujala, P., Haegebarth, A., Stange, D. E., Begthel, H., van den Born, M., Guryev, V., Oving, I. et al. (2009). Transcription factor achaete scute-like 2 controls intestinal stem cell fate. *Cell* **136**, 903-912.

van Es, J. H., van Gijn, M. E., Riccio, O., van den Born, M., Vooijs, M., Begthel, H., Cozijnsen, M., Robine, S., Winton, D. J., Radtke, F. et al. (2005). Notch/gamma-secretase inhibition turns proliferative cells in intestinal crypts and adenomas into goblet cells. *Nature* **435**, 959-963.

van Es, J. H., de Geest, N., van de Born, M., Clevers, H. and Hassan, B. A. (2010). Intestinal stem cells lacking the Math1 tumour suppressor are refractory to Notch inhibitors. *Nat. Commun.* **1**, 18.

VanDussen, K. L. and Samuelson, L. C. (2010). Mouse atonal homolog 1 directs intestinal progenitors to secretory cell rather than absorptive cell fate. *Dev. Biol.* **346**, 215-223.

Vooijs, M., Ong, C. T., Hadland, B., Huppert, S., Liu, Z., Korving, J., van den Born, M., Stappenbeck, T., Wu, Y., Clevers, H. et al. (2007). Mapping the consequence of Notch1 proteolysis in vivo with NIP-CRE. *Development* **134**, 535-544.

Wong, G. T., Manfra, D., Poulet, F. M., Zhang, Q., Josien, H., Bara, T., Engstrom, L., Pinzon-Ortiz, M., Fine, J. S., Lee, H. J. et al. (2004). Chronic treatment with the gamma-secretase inhibitor LY-411,575 inhibits beta-amyloid peptide production and alters lymphopoiesis and intestinal cell differentiation. *J. Biol. Chem.* **279**, 12876-12882.

Wu, Y., Cain-Hom, C., Choy, L., Hagenbeek, T. J., de Leon, G. P., Chen, Y., Finkle, D., Venook, R., Wu, X., Ridgway, J. et al. (2010). Therapeutic antibody targeting of individual Notch receptors. *Nature* **464**, 1052-1057.

Yang, Q., Bermingham, N. A., Finegold, M. J. and Zoghbi, H. Y. (2001). Requirement of Math1 for secretory cell lineage commitment in the mouse intestine. *Science* **294**, 2155-2158.

Zhang, J., Liu, W. L., Tang, D. C., Chen, L., Wang, M., Pack, S. D., Zhuang, Z. and Rodgers, G. P. (2002). Identification and characterization of a novel member of olfactomedin-related protein family, hGC-1, expressed during myeloid lineage development. *Gene* **283**, 83-93.

Zhang, X., Huang, Q., Yang, Z., Li, Y. and Li, C. Y. (2004). GW112, a novel antiapoptotic protein that promotes tumor growth. *Cancer Res.* **64**, 2474-2481.

Zhu, L., Gibson, P., Currle, D. S., Tong, Y., Richardson, R. J., Bayazitov, I. T., Poppleton, H., Zakharenko, S., Ellison, D. W. and Gilbertson, R. J. (2009). Prominin 1 marks intestinal stem cells that are susceptible to neoplastic transformation. *Nature* **457**, 603-607.

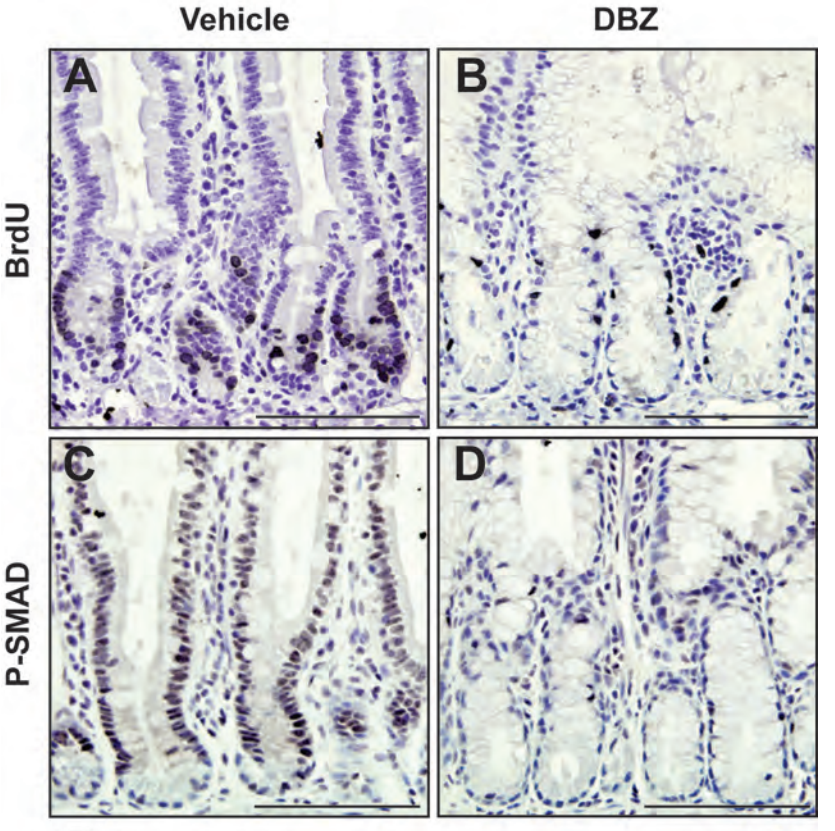
Vehicle
DBZ
A
B
C
D
BrdU
P-SMAD

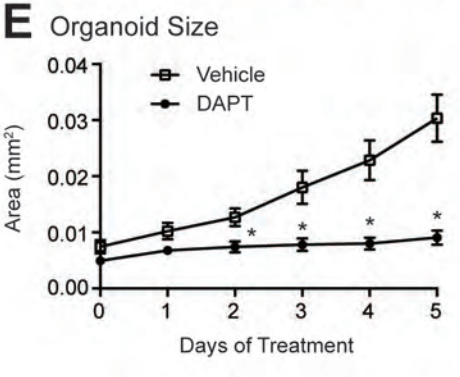
E
Organoid Size
Vehicle
DAPT
Area (mm²)
0.04
0.03
0.02
0.01
0.00
0
1
2
3
4
5
Days of Treatment
*
*
*
*

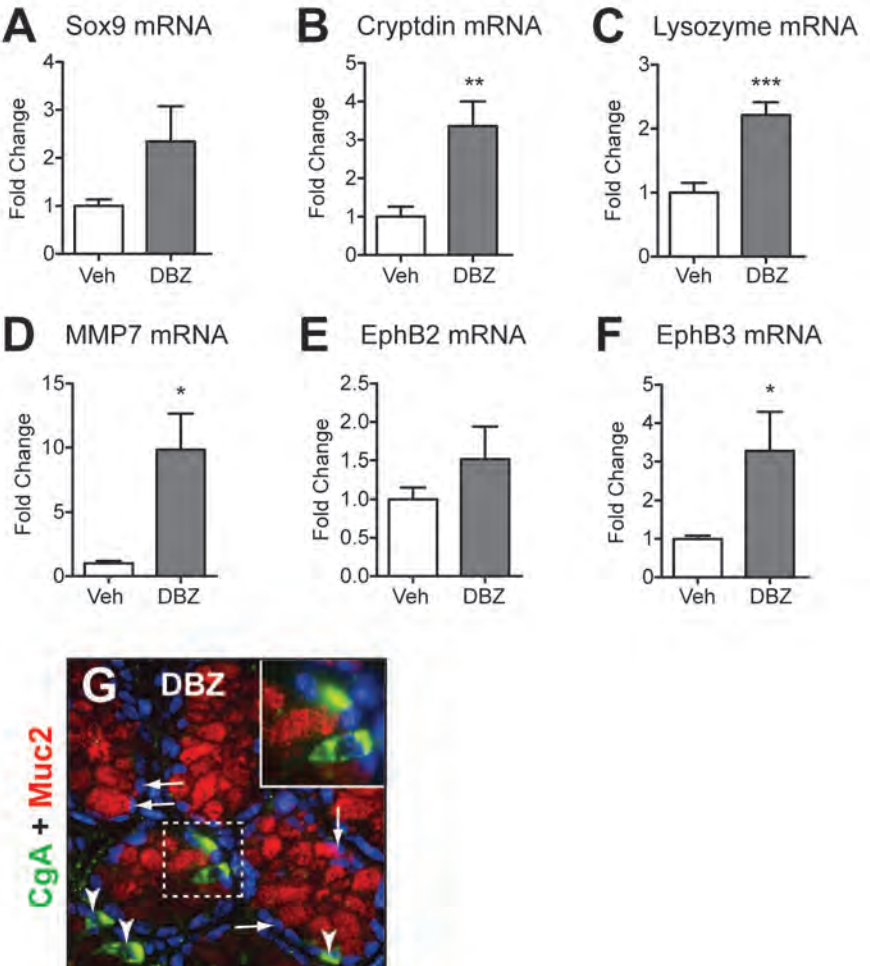
A
Sox9 mRNA
Fold Change
Veh
DBZ
B
Cryptdin mRNA
**
C
Lysozyme mRNA
***
D
MMP7 mRNA
*
E
EphB2 mRNA
F
EphB3 mRNA
G
DBZ
CgA + Muc2

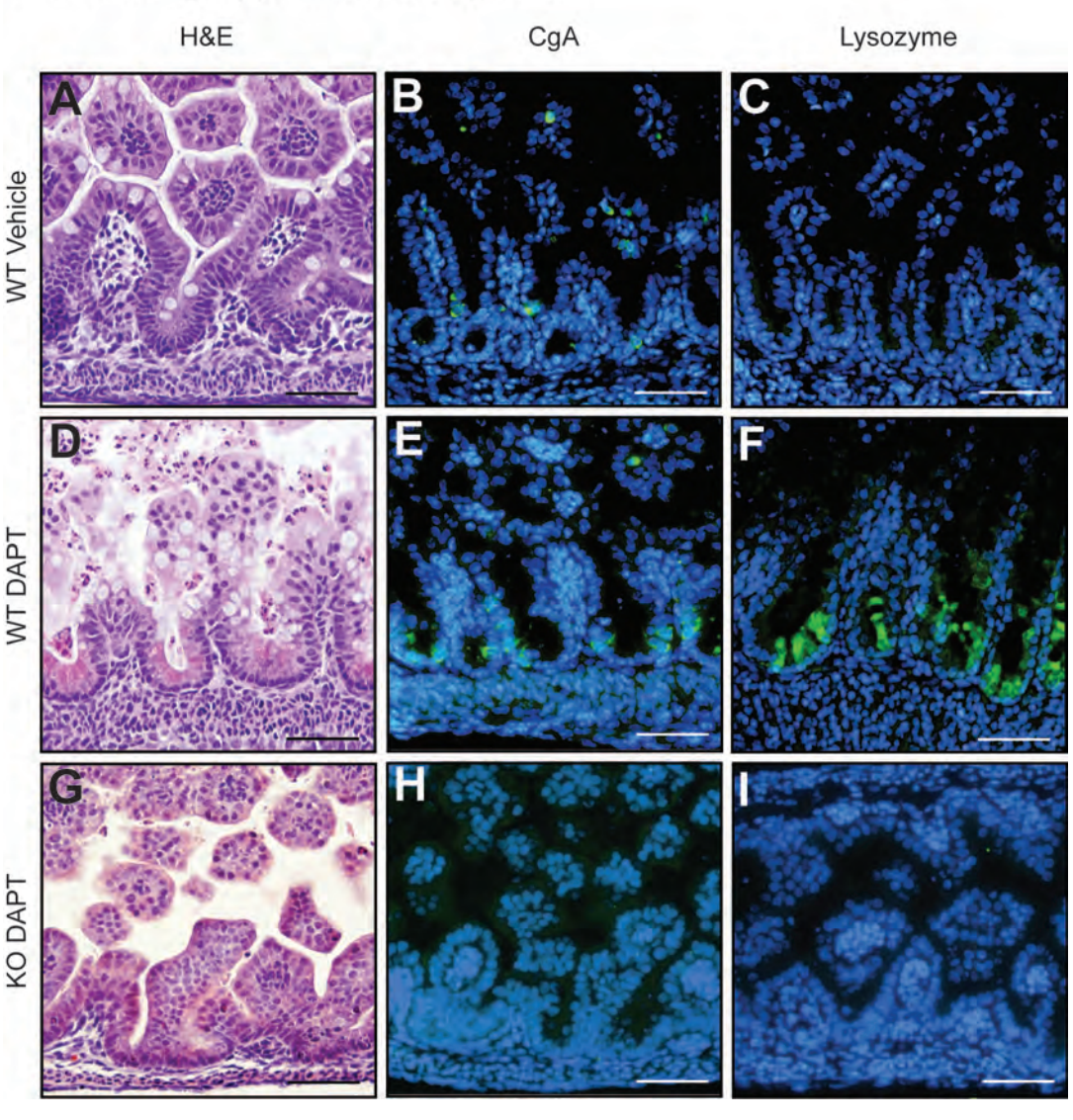
H&E
CgA
Lysozyme
WT Vehicle
WT DAPT
KO DAPT
A
B
C
D
E
F
G
H
I

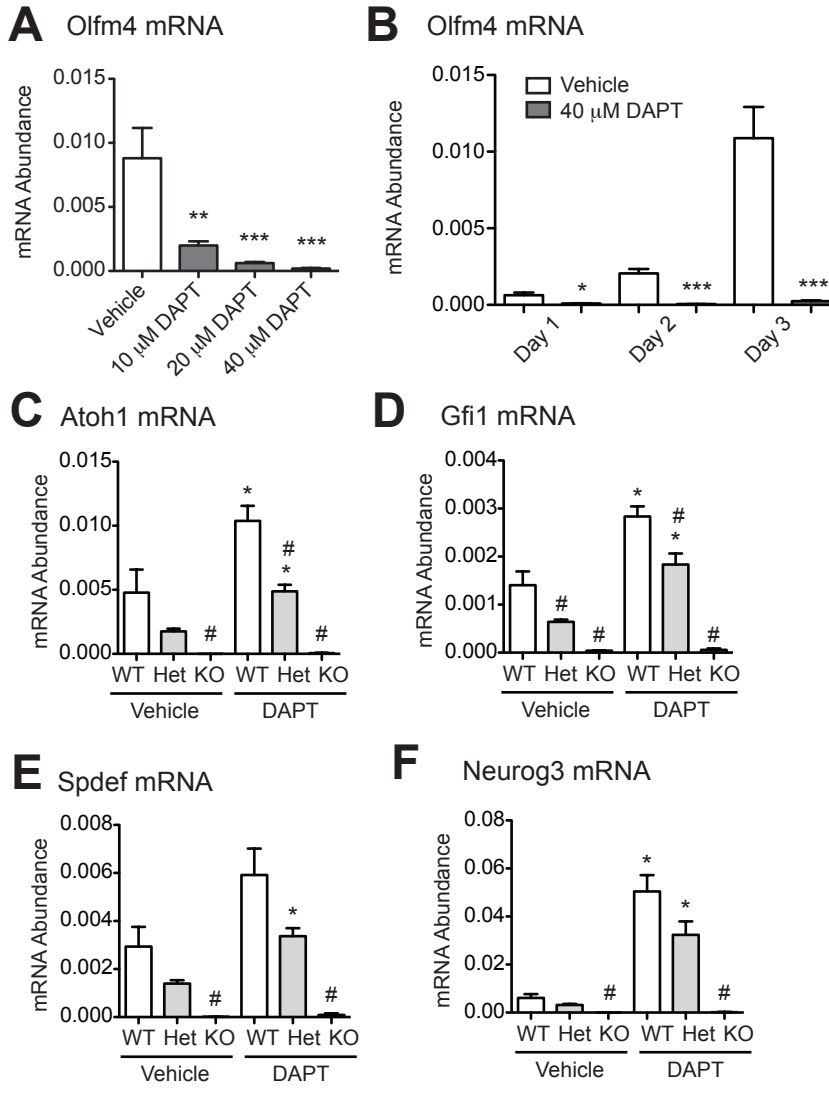
A
Olfm4 mRNA
mRNA Abundance
0.015
0.010
0.005
0.000
**
***
***
Vehicle
10 μM DAPT
20 μM DAPT
40 μM DAPT
B
Olfm4 mRNA
Vehicle
40 μM DAPT
mRNA Abundance
0.015
0.010
0.005
0.000
*
***
***
Day 1
Day 2
Day 3
C
Atoh1 mRNA
mRNA Abundance
0.015
0.010
0.005
0.000
*
#
*
#
WT Het KO WT Het KO
Vehicle
DAPT
D
Gfi1 mRNA
mRNA Abundance
0.004
0.003
0.002
0.001
0.000
*
#
*
#
#
WT Het KO WT Het KO
Vehicle
DAPT
E
Spdef mRNA
mRNA Abundance
0.008
0.006
0.004
0.002
0.000
*
#
#
WT Het KO WT Het KO
Vehicle
DAPT
F
Neurog3 mRNA
mRNA Abundance
0.08
0.06
0.04
0.02
0.00
*
*
#
#
WT Het KO WT Het KO
Vehicle
DAPT

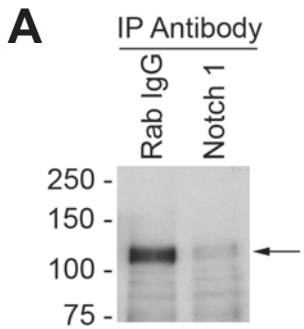

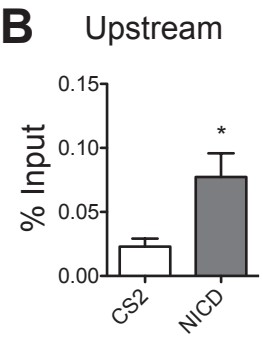

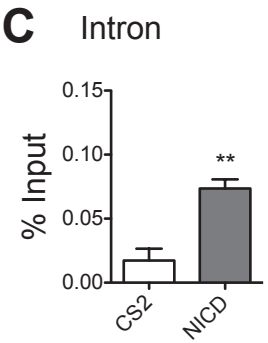

D Upstream Sequence

agaggctactagcaaatgagaacagatttgccatttgttttggtgggaat -1923
cgggaggaagaggggaattgtgctgggaggtagagacacattcttctcct
tatgtccatattcattgcattcaatcttagaataatggattcagtctccc
agttttcattctcacacattctgtatgcattccctgccttggactgggga
tctaagtggttagaacatttgaccaaagaggccaaggctgaactgcttcc
cacagagaacaatgaactttacagcccacatttctccctatctgttcttc
ttcactctctatccatccatttgtggttttcctgtctccccttccccctc
cccaccaccccagtttctgaatagtgtaccaggggtttaagaccctgttt
ctcacattagcactgtgcttattctgagagtttgtgtggagcttctgggg
tggggtggagtggggcatgaaccttctctccttgttttgaacccagcaat
cttacatattgatctagtctttaggaaattaaacaaacaatgaaaaagct
gacatttttatggcacgtcaaaagtcataagcaacttcccatacaatatt
tcatttaattcaaacaatttaggaattgttacaacctagaggggctaag
tgacatgctcaaggccaccgactcattgtgacacagctttttgtttgtt
tttgttcttttgagacagccttactctgtcacccatgctgcagtgcagtg
gtgtgaacatggctcactacagccgcaacctccaggctcaggtgatcct
cccacctcagcttcccaagtagctgggaccacaggtgcataccgccacac
ttggctatttttttcatttttgtagagacagggtctcaccacattgccc
aggatggtctccaactcttgagctcaagccatcctcccaccttggcctcc
caaagtgctgggattacaggtgcgagccagcatccccggcccagagctgg
gtcttaataccgagactaacacctttttctttctccagggaagaaggcag
aggtcacaaaggtgtgtgaaatgttgagcagggcaaatggatcctggagc
ccagggtcagagctgctgagcaagagaaaatgcatcttatttctcagttt -823

E Intron Sequence

gatgggaactgttagggaaagactctgtgagttgcagctctgggaagttt +678
gtccagttgttttgctgcctggcaggatcccggaatggtgaacagtagcc
ctcgagggagtgagagccgcagtgccctagttgaagccctgaccatttct
cttggcctggtttataaaggaggtgggtgtcagaaataaggggggagtta
ctggtctttagcaaagtgttattaccagtggacattcgcctaggggagtg
ttcactctttgcagtcttctttacagggaatcttcaggaccatttccagc
tccaaacaacagtagcaacaaacaaacaaaaccaaaagtcatgcattaca
acgaggctggtacagctaggctaagtgcattgaaggcatagtaagccagt
tccgtgggggatgagtcctctttggatctcctttaaagaaaggagaatgg
gctggagggcatgagaggttaggaggtaagaagcagttattcatttcact +1128

Table S1. Oligonucleotide sequences used for PCR genotyping

Strain	Primer (5′ to 3′)	Product
Atoh1$^{lacZ/lacZ}$	M1-F: TGCTGCATGCAGAAGAGTGGGCTGAGGTAA	374 bp (WT allele)
Atoh1$^{lacZ/lacZ}$	M1-R: TCAGCTTGCACAGCTGTTCCCGTACTTTGA	
Atoh1$^{lacZ/lacZ}$	lacZ-A: GCTGGGATCCGCCATTGTCAGACA	~300 bp (*lacZ* null allele)
Atoh1$^{lacZ/lacZ}$	lacZ-S: GCTGGAATTCCGCCGATACTG	
Vil-Cre	MVP5498-F: ACAGGCACTAAGGGAGCCAATG	
Vil-Cre	MVP6378-R: GATTCAGGTCAGAAAGAGGTCACAG	881 bp (WT allele), ~350 bp (Cre allele)
Vil-Cre	CreORF-R2: GTTCTTGCGAACCTCATCACT	

Table S2. Oligonucleotide sequences used for qRT-PCR

Gene	Forward primer (5′ to 3′)	Reverse primer (5′ to 3′)
Ascl2	CCTCTCTCGGACCCTCTCTCAG	CAGTCAAGGTGTGCTTCCATGC
Atoh1	GCCTTGCCGGACTCGCTTCTC	TCTGTGCCATCATCGCTGTTAGGG
cryptdins	AGGAGCAGCCAGGAGAAG	ATGTTCAGCGACAGCAGAG
Ephb2	ATGCTGAAGAAGTGGATG	CTTGAAGGTTCCTGATGG
Ephb3	AAGAGACTCTCATGGACACGAAAT	ACTTCCCGCCGCCAGATG
Gapdh	TCAAGAAGGTGGTGAAGCAGG	TATTATGGGGGTCTGGGATGG
*GAPDH**	GAGTCCACTGGCGTCTTCACC	GAGGCATTGCTGATGATCTTGAGG
Gfi1	TCGTCCGAGTTCGAGGACTT	CAGAGAGCGGCACAGTGACTT
GFP	ACCCTCGTGACCACCCTGACC	TGCCGTCGTCCTTGAAGAAGATGG
Lgr5	CGAGCCTTACAGAGCCTGATACC	TTGCCGTCGTCTTTATTCCATTGG
lysozyme	ATGGAATGGCTGGCTACTATGGAG	CTCACCACCCTCTTTGCACATTG
Mmp7	CAGACTTACCTCGGATCGTAGTGG	GTTCACTCCTGCGTCCTCACC
Neurog3	ACCCTATCCACTGCTGCTTGTC	CGGGAAAAGGTTGTTGTGTCTCTG
Olfm4	GCCACTTTCCAATTTCAC	GAGCCTCTTCTCATACAC
*OLFM4**	TTCTCCTAGCCCTTCTGTTCTTCC	TTCCAAGCGTTCCACTCTGTCC
Prom1	CACTCCTGACTGAAACACCAAAGC	TGCCATCCAGGTCTGAGAATGC
Sox9	CTGGAGGCTGCTGAACGAGAG	CGGCGGACCCTGAGATTGC
Spdef	GGACGGACGACTCTTCTGACAG	GCTCCTGATGCTGCCTTCTCC

*Sequences designed to amplify the human gene; all other primers amplify the mouse gene.

Table S3. Oligonucleotide sequences used to generate the mutant human *OLFM4* constructs

Nucleotides deleted	Primer sequence (5′ to 3′)
–427 to –306	Forward: TGTGCTGGAATTCGCCTCTGTGTCATCCAC
	Reverse: GTGGATGACACAGAGGCGAATTCCAGCACA
–290 to –160	Forward: CTCTGTGTCATCCACCCTCACTGACAAGGT
	Reverse: ACCTTGTCAGTGAGGGTGGATGACACAGAG
–145 to –56	Forward: CCTCACTGACAAGGTCATGGGGAAATCACC
	Reverse: GGTGATTTCCCCATGACCTTGTCAGTGAGG
–249 to –244 (RBPJa)	Forward: CTCTTTCAAGGAAGTACCAAGACCAAATATTGGGCTTTACAA
	Reverse: TTGTAAAGCCCAATATTTGGTCTTGGTACTTCCTTGAAAGAG
–101 to –89 (RBPJb)	Forward: GAACCTCCTGGGGCCCTGGCCACTCC
	Reverse: GGAGTGGCCAGGGCCCCAGGAGGTTC

Table S4. Oligonucleotide sequences used for quantitative PCR analysis of ChIP

Gene (primer location*)	Forward primer (5′ to 3′)	Reverse primer (5′ to 3′)
OLFM4 (–146 to –128)	TGTGGGCCATGACTCAGATTCC	TATAGTGCCCAGTGGTGATTTCCC
OLFM4 (–1337 to –1190)	CCTAGAGGGGCTAAGTGACATGC	GGAGGTTGCGGCTGTAGTGAG
OLMF4 (–11961 to –11783)	CAGTGGCAATGGAAAACTGA	CAGCTTTGCCCTCTTTACCA
OLFM4 (+917 to +1087)	ACCATTTCCAGCTCCAAACAACAG	CCCTCCAGCCCATTCTCCTTTC
HES1‡ (–105 to +67)	CCTCCCATTGGCTGAAAGTTACTG	AGGACCAAGGAGAGAGGTAGACG

*The location of the PCR product is presented as the number of base pairs relative to the transcription start site of the appropriate gene.
‡Consensus RBPJκ binding sites are located in the *HES1* promoter at –83 to –76 and –59 to –52 relative to the transcription start site.